Superlattices and Microstructures 122 (2018) 548–556

Contents lists available at ScienceDirect

Superlattices and Microstructures

journal homepage: www.elsevier.com/locate/superlattices

Spin relaxation mediated by spin-orbit and acoustic phonon interactions in a single-electron two-dimensional quantum dot

A.L. Vartanian, A.A. Kirakosyan, K.A. Vardanyan*

Department of Solid State Physics, Yerevan State University, 1, A.Manoogian, 0025, Yerevan, Armenia

A B S T R A C T

The spin relaxation caused by both spin-orbit and electron-acoustic phonon interactions in a two-dimensional quantum dot embedded into nanosize semiconductor slabs in a perpendicular magnetic field is studied. The spin relaxation rate due to electron coupling to both dilatational and flexural acoustic phonon modes is analytically and numerically evaluated. It is shown that the magnetic field dependency of the spin relaxation rate has allowed and forbidden regions and it can change in a very large region depending on magnetic field. The obtained results show that by means of gate-voltage it is possible to realize the confinement, which makes the required transition rate between certain states available.

1. Introduction

Semiconductor nanostructures have become an appealing material system for spintronics and quantum technologies due to their intriguing electronic and optical properties and connectivity with other semiconductor hardware [1]. Manipulation and readout of spins in solids offer a powerful route towards quantum computation [2,3] and prominent device proposals such as the spin-field-effect transistor [4] and spin-polarized p-n junctions [5]. To achieve spin-based semiconductor electronics, long spin coherence or long relaxation length should be required. Therefore, the main challenge is to find materials and construct semiconductor nanostructures for which the carriers' spin relaxation and coherence times are long enough to control individual spins and measure the spin of an individual electron. The three-dimensional confinement in a quantum dots (QDs) quantizes energies of quasi-particles and leads to long coherence times of confined charges and spins [6,7] and experimental control of electronic spins in QDs [8]. A single electron spin in a QD has been detected using magnetic resonance force microscopy [9]. Moreover, the readout of an electron spin in a QD via pulsed relaxation measurements [10] and optical orientation experiments [11] have been reported. QDs have been proposed as a host for a quantum bit (qubit), which is the quantum analog of the binary bit in a classical digital computer, where the spin of an electron located in the QD forms the fundamental two-level system of a qubit, which is essentially controllable. Electrical control instead of magnetic one is particularly appealing for this purpose, because electric fields are easy to generate locally on-chip. Coherent control of a single electron spin in a quantum dot using an oscillating electric field generated by a local gate has been experimentally realized [12]. Coupling of the electric field to the spins is mediated by the spin-orbit (SO) interaction naturally provided by the semiconductor host environment. It has been shown [12] that the electrically induced spin transitions were mediated by the SO interaction.

The environment can strongly affect on the relaxation characteristics of a quantum system. Therefore, the understanding of the dominant dissipation mechanisms allows us to point at strategies for minimizing relaxation, and thereby improving coherent control of quantum systems. The dominant source of dissipation in dots is the interaction with phonons [13–23]. The SO coupling leads to spin admixture [[13–15] [19–23]] and thus allowing transitions between states of opposite spin. The dissipation by phonons is

* Corresponding author.
E-mail addresses: vardan@ysu.am (A.L. Vartanian), kirakosyan@ysu.am (A.A. Kirakosyan), karvard@ysu.am (K.A. Vardanyan).

https://doi.org/10.1016/j.spmi.2018.06.053
Received 9 May 2018; Received in revised form 23 June 2018; Accepted 24 June 2018
Available online 27 June 2018

needed to comply with energy conservation. Thus the SO coupling allows spin relaxation mediated by phonons. Also, the phonon can, under certain conditions, induce spin dependent coupling to the electron called direct spin-phonon coupling [13,14,18,19]. The phonon in anisotropic environment induces electric field similar to electric field arising due to structural inversion asymmetry caused by the confinement (Rashba term). In particular, it has been experimentally shown [10,11,16,17,20] that the spin-acoustic phonon coupling is a dominant spin relaxation mechanism in GaAs quantum dots in strong magnetic fields ($B > 1$ T). The acoustic phonon-induced spin relaxation in a two-dimensional QD, without inclusion of phonon confinement effect, has been theoretically considered in Ref. [22].

The control of vibrational properties of quantum dots is important for the improvement of the coherence of spin qubits in quantum dot. Such control can be successfully realized in a single QD embedded into a free-standing structure (semiconductor slab). There are various fabrication techniques and applications of such structures. Electron beam evaporation [24], molecular beam epitaxy [25] and standard lithographic techniques [26] have made possible the fabrication of free-standing layers (quantum wells) with a few-nanometer thickness. Such quantum well is used as a model for a nano-size planar phonon cavity. In unstrained quantum slab, acoustic and optical phonon dispersions change due to spatial confinement induced by the free surface boundaries. As a result, new phonon modes essentially differ from the usual bulk modes. There are three types of acoustic modes: shear, dilatational and flexural, which are experimentally controllable. All these modes couple to the electric charge and, in principle, all of them couple also to the spin of single electron in quantum dot.

In this paper, the effect of phonon confinement on spin relaxation due to electron–acoustic-phonon scattering and spin-orbit coupling is investigated in a two-dimensional quantum dot embedded into a free-standing semiconductor slab. We present a systematic study of the spin relaxation rate of a single electron to manipulate the mixing of the spin and orbital states by using gate-voltages.

The structure of the paper is as follows: In Sec. 2, we introduce the electron states in two-dimensional quantum dot in magnetic field by taking into account the spin-orbit coupling. Acoustical phonon modes and electron-phonon interaction Hamiltonian in frame of deformation potential in free-standing semiconductor slab are presented in Sec. 3. In Sec. 4, we derive the phonon mediated spin relaxation rate in two-dimensional quantum dot in the presence of a magnetic field. Finally, in Sec. 5, we discuss the implications of our results on spin relaxation rate, and give our conclusions.

2. Electron states in two-dimensional quantum dot in magnetic field with spin-orbit coupling

We consider single electron two-dimensional quantum dot with parabolic confinement potential embedded in an infinite semiconductor slab of thickness d. The single-electron Hamiltonian in the presence of SO interaction is given by $H = H_0 + H_{SOI}$ with

$$H_0 = \frac{\boldsymbol{P}^2}{2m^*} + \frac{m^*\omega_0^2}{2}(x^2 + y^2) + \frac{1}{2}g^*\mu_B B\sigma_z, \tag{1}$$

$$H_{SOI} = \boldsymbol{\sigma\Omega}(\boldsymbol{P}), \tag{2}$$

where $\boldsymbol{P} = -i\hbar\nabla + e\boldsymbol{A}$ is the quasimomentum of electron, e is the elementary charge, the vector potential $\boldsymbol{A} = (B/2)(-y, x.0)$ describes a magnetic field $\boldsymbol{B}$ perpendicular to the semiconductor slab, m^* is the electron effective mass in the conduction band, ω_0 is the characteristic confinement frequency, g^* is the electron bulk g-factor, μ_B is the Bohr magneton, $\boldsymbol{\sigma}(\sigma_x,\ \sigma_y,\ \sigma_z)$ is the vector of the Pauli matrices, $\boldsymbol{\Omega}$ is the Larmor precession frequency vector corresponding to the precession of the electron spin about magnetic field caused by the spin-orbit interaction. The key sources of spin-orbit interaction in a 2D electron system are the crystals' lack of inversion symmetry (bulk inversion asymmetry) and the structural inversion asymmetry. Therefore the precession frequency vector can be represented as $\boldsymbol{\Omega}(\boldsymbol{P}) = \boldsymbol{\Omega}_D(\boldsymbol{P}) + \boldsymbol{\Omega}_R(\boldsymbol{P})$, where $\boldsymbol{\Omega}_D(\boldsymbol{P}) = \beta_D(-P_x, P_y, 0)$ is the bulk inversion asymmetry or Dresselhaus term, $\boldsymbol{\Omega}_R(\boldsymbol{P}) = \alpha_R(P_y, -P_x, 0)$ is the structural inversion asymmetry or Rashba term. The Dresselhaus term is taken linear with respect to the electron quasimomentum $\boldsymbol{P}$, and β_D (α_R) is the Dresselhaus (Rashba) parameter.

Following Ref. [22], we introduce phase coordinates $(r_1,\ r_2,\ p_1,\ p_2)$ which connected to the previous ones $(x,\ y,\ p_x,\ p_y)$ by the following formula

$$x = \frac{1}{\sqrt{2\omega}}(\sqrt{\omega_1}r_1 + \sqrt{\omega_2}r_2),\quad y = \frac{1}{m^*\sqrt{2\omega}}\left(\frac{p_1}{\sqrt{\omega_1}} - \frac{p_2}{\sqrt{\omega_2}}\right), \tag{3}$$

$$p_x = \frac{\sqrt{\omega}}{\sqrt{2}}\left(\frac{p_1}{\sqrt{\omega_1}} + \frac{p_2}{\sqrt{\omega_2}}\right),\ p_y = \frac{m^*\sqrt{\omega}}{\sqrt{2}}(-\sqrt{\omega_1}r_1 + \sqrt{\omega_2}r_2), \tag{4}$$

Where

$$\omega = \sqrt{\omega_0^2 + \frac{\omega_c^2}{4}}\ ,\ \omega_c = \frac{eB}{m^*}\ ,\ \omega_{1,2} = \omega \mp \frac{\omega_c}{2}. \tag{5}$$

r_1, r_2, p_1, and p_2 fulfill the commutation relations

$$[p_1, r_1] = [p_2, r_2] = -i\hbar,\ [p_2, r_1] = [p_1, r_2] = [p_1, p_1] = [p_2, p_2] = [r_1, r_1] = [r_2, r_2] = 0. \tag{6}$$

Then, the eigenstates and the energy spectrum of electrons in a QD without the SO coupling are given by the expressions

$$\Psi_{n,s,\sigma}(r_1, r_2) = \frac{1}{\sqrt{\sqrt{\pi}\,2^n n!\, L_{\omega_1}}\sqrt{\sqrt{\pi}\,2^s s!\, L_{\omega_2}}} e^{-\frac{1}{2}\left(\frac{r_1}{L_{\omega_1}}\right)^2} \mathrm{H}_n\left(\frac{r_1}{L_{\omega_1}}\right) e^{-\frac{1}{2}\left(\frac{r_2}{L_{\omega_2}}\right)^2} \mathrm{H}_s\left(\frac{r_2}{L_{\omega_2}}\right)\chi_\sigma, \tag{7}$$

$$E_{n,s,\sigma} = \hbar\omega_1\left(n + \frac{1}{2}\right) + \hbar\omega_2\left(s + \frac{1}{2}\right) + g^*\mu_B B\sigma, \tag{8}$$

where n, s = 0,1,2, ..., $\sigma = \pm 1/2$, $L_{\omega_{1,2}} = \sqrt{\hbar/m^*\omega_{1,2}}$, $\mathrm{H}_n(x)$ are the Hermite polynomials of integer order n, $\chi_{1/2} = \begin{pmatrix}1\\0\end{pmatrix} \equiv \uparrow$, and $\chi_{-1/2} = \begin{pmatrix}0\\1\end{pmatrix} \equiv \downarrow$ are the spinors for up- and down-spin projected in the z direction, respectively.

The Rashba and Dresselahaus terms in Eq. (2) can be expressed in terms of the new variables as

$$\boldsymbol{\sigma\Omega_R}(\boldsymbol{P}) = \alpha_R\left[\sigma_x m^*\left(-r_1\frac{\omega_1^{3/2}}{\sqrt{2\omega}} + r_2\frac{\omega_2^{3/2}}{\sqrt{2\omega}}\right) + i\hbar\sigma_y\left(\frac{\omega_1^{1/2}}{\sqrt{2\omega}}\frac{\partial}{\partial r_1} + \frac{\omega_2^{1/2}}{\sqrt{2\omega}}\frac{\partial}{\partial r_2}\right)\right], \tag{9}$$

$$\boldsymbol{\sigma\Omega_D}(\boldsymbol{P}) = \beta_D\left[\sigma_y m^*\left(-r_1\frac{\omega_1^{\frac{3}{2}}}{\sqrt{2\omega}} + r_2\frac{\omega_2^{\frac{3}{2}}}{\sqrt{2\omega}}\right) + i\hbar\sigma_x\left(\frac{\omega_1^{\frac{1}{2}}}{\sqrt{2\omega}}\frac{\partial}{\partial r_1} + \frac{\omega_2^{\frac{1}{2}}}{\sqrt{2\omega}}\frac{\partial}{\partial r_2}\right)\right]. \tag{10}$$

For a GaAs QD the SO lengths $l_R = \hbar/m^*\alpha_R$, and $l_D = \hbar/m^*\beta_D$ are of order of $8\mu m$ and are much larger than the hybrid orbital length $L_\omega = \sqrt{\hbar/m^*\omega}$ of a QD. Therefore, the SO terms can be considered as small perturbations [22,27] which cause the transitions between different eigenstates of H_0.

With the use of relations

$$\sigma_x\chi_{1/2} = \chi_{-1/2},\quad \sigma_x\chi_{-1/2} = \chi_{1/2},\quad \sigma_y\chi_{1/2} = i\chi_{-1/2},\quad \sigma_x\chi_{-1/2} = -i\chi_{1/2}, \tag{11}$$

the transition matrix elements between different orbital states can be found as

$$<\Psi_{n,t,\downarrow}|H_{SO}^R|\Psi_{p,s,\uparrow}> = \hbar\alpha_R L_\omega(-L_{\omega_1}^{-2}\sqrt{p}\,\delta_{t,s}\delta_{n,p-1} + L_{\omega_2}^{-2}\sqrt{s+1}\,\delta_{t,s+1}\delta_{n,p}), \tag{12}$$

$$<\Psi_{n,t,\uparrow}|H_{SO}^R|\Psi_{p,s,\downarrow}> = \hbar\alpha_R L_\omega(-L_{\omega_1}^{-2}\sqrt{p+1}\,\delta_{t,s}\delta_{n,p+1} + L_{\omega_2}^{-2}\sqrt{s}\,\delta_{t,s-1}\delta_{n,p}), \tag{13}$$

$$<\Psi_{n,t,\downarrow}|H_{SO}^D|\Psi_{p,s,\uparrow}> = i\hbar\beta_D L_\omega(-L_{\omega_1}^{-2}\sqrt{p+1}\,\delta_{t,s}\delta_{n,p+1} + L_{\omega_2}^{-2}\sqrt{s}\,\delta_{t,s-1}\delta_{n,p}), \tag{14}$$

$$<\Psi_{n,t,\uparrow}|H_{SO}^D|\Psi_{p,s,\downarrow}> = -i\hbar\beta_D L_\omega(-L_{\omega_1}^{-2}\sqrt{p}\,\delta_{t,s}\delta_{n,p-1} + L_{\omega_2}^{-2}\sqrt{s+1}\,\delta_{t,s+1}\delta_{n,p}). \tag{15}$$

Spin-flip transitions are caused by spin-orbit interaction due to the mixing of the spin states. The mixing determines an effective g-factor and its anisotropy as a function of the magnetic field orientation [28].

2.1. Acoustical phonon modes and electron-phonon interaction Hamiltonian in free-standing semiconductor slab

It is well known that the acoustic phonon modes in the approximation of a homogenous medium in a free-standing semiconductor layer are classified as shear, dilatational and flexural ones [29]. The vector of relative displacement for shear modes has only component perpendicular to the propagation direction; thus, shear modes are similar to the transverse waves in bulk material. The symmetries of displacement fields of dilatational and flexural modes differ with respect to the midplane of the slab. For dilatational (or symmetrical) modes, the displacement vector $\boldsymbol{U}$ has two non-zero components: $\boldsymbol{U}(\boldsymbol{q}, z) = (U_x, 0, U_z)$,

$$\begin{aligned} U_x &= iq_x\left[(q_x^2 - q_t^2)sin\tfrac{q_t d}{2}cosq_l z + 2q_l q_t sin\tfrac{q_l d}{2}cosq_t z\right],\\ U_z &= q_l\left[-(q_x^2 - q_t^2)sin\tfrac{q_t d}{2}sinq_l z + 2q_x^2 sin\tfrac{q_l d}{2}sinq_t z\right], \end{aligned} \tag{16}$$

where the x axis is directed along $\boldsymbol{q}$ i.e. $\boldsymbol{q}(q_x, 0)$. The q_l and q_t parameters are determined by the equations

$$\frac{\tan(q_t d/2)}{\tan(q_l d/2)} = -\frac{4q_x^2 q_l q_t}{(q_x^2 - q_t^2)^2}, \tag{17}$$

Where $s_l = \sqrt{(\lambda + 2\mu)/\rho}$ and $s_t = \sqrt{\mu/\rho}$ are the longitudinal and transversal velocities of the acoustic waves in solid media, respectively, λ and μ are the Lame constants of the medium, ρ is the material density. For a given value of q_x, these equations have many solutions and they are numbered with the additional index n i.e. $q_{l,n}$ and $q_{t,n}$ (these solutions may be real or complex depending on the value of q_x). The frequencies of the dilatational waves are given by the relation

$$\omega_n = s_l\sqrt{q_x^2 + q_{l,n}^2} = s_t\sqrt{q_x^2 + q_{t,n}^2}\,. \tag{19}$$

For flexural (or antisymmetric) modes, the displacement vector $\boldsymbol{U}$ has two nonzero components: U_x and U_z, which are given by the following expressions:

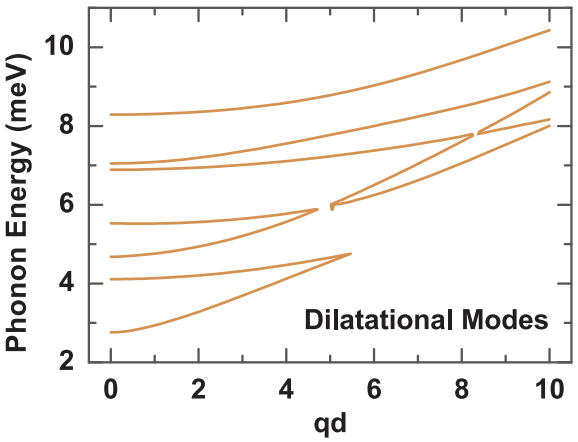

Fig. 1. The dependencies of dilatational (a) and flexural (b) acoustic phonon energies in free-standing GaAs quantum-well on in-plane wave vector ($d = 2$ nm).

$$U_x = iq_x\left[(q_x^2 - q_t^2)cos\frac{q_t d}{2}sinq_l z + 2q_l q_t cos\frac{q_l d}{2}sinq_t z\right],$$
$$U_z = q_l\left[(q_x^2 - q_t^2)cos\frac{q_t d}{2}cosq_l z + 2q_x^2 cos\frac{q_l d}{2}cosq_t z\right], \tag{20}$$

where the $q_{t,n}$ and $q_{l,n}$ parameters are determined from the following dispersion relation:

$$\frac{\tan(q_l d/2)}{\tan(q_t d/2)} = -\frac{4q_x^2 q_l q_t}{(q_x^2 - q_l^2)^2}. \tag{21}$$

The dependencies $q_{t,n}(q_x)$ and $q_{l,n}(q_x)$ for the dilatational and flexural modes makes it possible to calculate the dispersion curves for these modes. In Fig. 1 these curves are shown in the energy interval from 0 to 10 meV for the semiconductor layer of thickness $d = 2$ nm. Note that for flexural modes, the dispersion relation coincides with the expression given by (19), but it does not lead to the same frequencies, since for these modes $q_{t,n}$ and $q_{l,n}$ are different.

Actually, the displacement fields and phonon dispersions in free-standing layer strongly differ in vibrational properties from the bulk material. In the first one, the confinement leads to phonon quantization into subbands. The second situation is that, in contrast to the isotropic crystal where the longitudinal and transversal polarizations are separated, the boundary conditions at the surface of free-standing layer lead to coupling between longitudinal and transversal acoustic modes.

For electron-phonon coupling, the deformation potential is supposed to be the main contributor in our model. For phonon modes which are allowed to effect, only dilatational waves and flexural waves are contributive. Shear waves are neglected because their interaction with electrons vanishes.

The electron interaction Hamiltonian with the dilatational and flexural acoustic phonon modes in the deformation potential approximation is given by the expression [29].

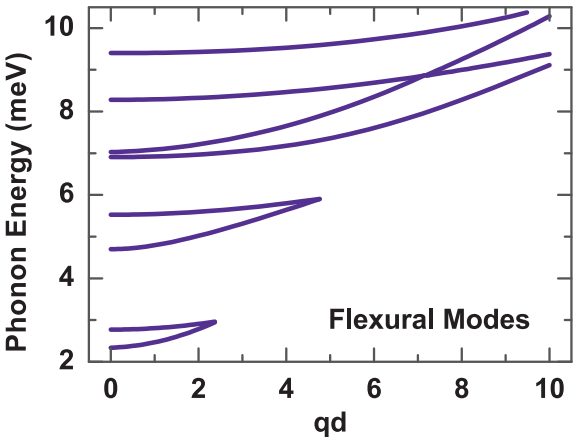

Fig. 1. (*continued*)

$$H_{el-ph}^{ac} = \sum_{\beta,n,\boldsymbol{q}} e^{iqx}\Gamma_{\beta}(\boldsymbol{q}, n, z)[c_{n\beta}(\boldsymbol{q}) + c_{n\beta}^{+}(-\boldsymbol{q})], \tag{22}$$

where $c_{n\beta}^{+}(c_{n\beta}(\boldsymbol{q}))$ are the creation (annihilation) operator of the dilatational ($\beta = d$) and the flexural ($\beta = f$) phonons characterized by the in-plane wave vector $\boldsymbol{q}$ and the branch n,

$$\Gamma_{\beta}(\boldsymbol{q}, n, z) = F_{\beta,n}\sqrt{\frac{\hbar E_a^2}{2A\rho\omega_n^{\beta}(\boldsymbol{q})}}\left[(q_{t,n}^2 - q^2)(q_{l,n}^2 + q^2)tsc1_{\beta}\left(\frac{q_{t,n}d}{2}\right)tsc2_{\beta}(q_{l,n}z)\right], \tag{23}$$

E_a is the deformation potential constant, $tsc1_{\beta} = sin$, $tsc2_{\beta} = cos$ for $\beta = d$ and $tsc1_{\beta} = cos$, $tsc2_{\beta} = sin$ for $\beta = f$. The expressions of the normalization coefficients $F_{\beta,n}$ are given in Ref. [29].

2.2. Phonon mediated spin relaxation in two-dimensional quantum dot in magnetic field

Transitions from the excited states (0,0, ↓) and (0,1, ↓) to the ground state (0,0, ↑) without interaction with acoustic phonons are forbidden due to the requirement for energy conservation. We also note that the matrix elements of the Rashba and Dresselhaus interactions between (0,0, ↓) and (0,0, ↑) states, as follows from equations (12) and (14), are also zero. Hence, transitions from both the first excited state and the state (0,1, ↓) to the ground state must be considered in the second approximation of perturbation theory. Therefore, the second order perturbative calculation is performed for the electron spin relaxation via dilatational and flexural acoustic phonon modes in two-dimensional quantum dot. The probability per unit time to transit from initial state (n, t, σ) to final state (l, k, σ') by absorbing (+) or emitting (−) the acoustic phonon with energy $\hbar\omega_n^{\beta}(\boldsymbol{q})$ can be written as

$$W_{D(R)}^{\pm}(n, t, \sigma \to l, k, \sigma') = \frac{2\pi}{\hbar}\sum_{\beta,n,\boldsymbol{q}}^{p,s,\sigma'} \frac{|<\Psi_{n,t,\sigma}|H_{SO}^{D(R)}|\Psi_{p,s,\sigma'}>|^2 \left|<\Psi_{p,s,\sigma'}|H_{el-ph}^{ac,\ \beta,n,\boldsymbol{q}}|\Psi_{l,k,\sigma'}^{\pm}>\right|^2}{(E_{n,t,\sigma} - E_{p,s,\sigma'})^2} \times \delta(E_{l,k,\sigma'} - E_{n,t,\sigma} \pm \hbar\omega_n^{\beta}(\boldsymbol{q})). \tag{24}$$

The spin relaxation rate can be expressed as

$$\Gamma = \sum_{\pm} W^{\pm}(n, t, \sigma \to l, k, \sigma'). \tag{25}$$

The matrix element of the electron-acoustic phonon interaction can be written as

$$<\Psi_{p,s,\sigma'}|H_{el-ph}^{ac,\ \beta,n,\boldsymbol{q}}|\ \Psi_{l,k,\sigma'}>^{\pm} = \Gamma_{\beta}^{\pm}(\boldsymbol{q}, n)G_{\beta}(q_{l,n})\left\langle \Psi_{p,s,\sigma'}\left|e^{\frac{iq}{\sqrt{2\omega}}(\sqrt{\omega_1}r_1+\sqrt{\omega_2}r_2)}\right|\Psi_{l,k,\sigma'}\right\rangle, \tag{26}$$

where

$$\Gamma_{\beta}^{\pm}(\boldsymbol{q}, n) = \sqrt{\frac{\hbar E_a^2}{2A\rho\omega_n^{\beta}(\boldsymbol{q})}}F_{\beta,n}\left[(q_{t,n}^2 - q^2)(q_{l,n}^2 + q^2)tsc1_{\beta}\left(\frac{q_{t,n}d}{2}\right)\right]\sqrt{N_n^{\beta}(\boldsymbol{q}) + \frac{1}{2} \pm \frac{1}{2}}, \tag{27}$$

$N_n^{\beta}(\boldsymbol{q})$ is the phonon distribution function

$$G_{\beta}(q_{l,n}) = \int_0^{\infty}|\eta_0(z)|^2 tsc2_{\beta}(q_{l,n}z)dz. \tag{28}$$

In Eq. (28) $\eta_0(z)$ is the electron wave function in the inversion layer in quantum limit [30].
It is easy to show that in general case

$$\left\langle \Psi_{p,s,\sigma'}\left|e^{\frac{iq}{\sqrt{2\omega}}(\sqrt{\omega_1}r_1+\sqrt{\omega_2}r_2)}\right|\Psi_{l,k,\sigma'}\right\rangle = Q_{p,l}\left(\frac{qL_{\omega}}{\sqrt{2}}\right)Q_{s,k}\left(\frac{qL_{\omega}}{\sqrt{2}}\right), \tag{29}$$

where

$$Q_{p,l}(a) = \frac{1}{\sqrt{\pi}\sqrt{2^{p+l}p!l!}}\int_{-\infty}^{\infty} e^{-x^2}\mathrm{H}_p(x)e^{iax}\mathrm{H}_l(x)dx. \tag{30}$$

Thus

$$W_{D(R)}^{\pm}(n, t, \sigma \to l, k, \sigma') = \frac{2\pi}{\hbar}\sum_{\beta,n,q}^{p,s,\sigma'} \frac{|<\Psi_{n,t,\sigma}\ |\ H_{SO}^{D(R)}\ |\ \Psi_{p,s,\sigma'}>|^2 \left|\Gamma_{\beta}^{\pm}(\boldsymbol{q}, n)G_{\beta}(q_{l,n})\right|^2}{(E_{n,t,\sigma} - E_{p,s,\sigma'})^2} \times \left|Q_{p,l}\left(\frac{qL_{\omega}}{\sqrt{2}}\right)Q_{s,k}\left(\frac{qL_{\omega}}{\sqrt{2}}\right)\right|^2 \delta(E_{l,k,\sigma'} - E_{n,t,\sigma} \pm \hbar\omega_n^{\beta}(\boldsymbol{q})). \tag{31}$$

Let us now consider the contributions of transitions from the states $|00\downarrow$ and $|01\uparrow$ to the ground state for both Rashba and Dresselhaus, and its joint influence. Using the expressions (12)–(15) of matrix elements it easy to determine that the transition from

the state $|00\downarrow$ to the state $|00\uparrow$ due to Rashba and Dresselhaus SO interactions is realized via mediate states $|1,\ 0,\uparrow$ and $|0,1,\uparrow$, respectively.

Because of

$$<\Psi_{0,0,\downarrow}\ |H_{SO}^{R}|\ \Psi_{1,0,\uparrow}> = -\hbar\alpha_R L_\omega L_{\omega_1}^{-2}, \qquad <\Psi_{0,0,\downarrow}\ |H_{SO}^{D}|\ \Psi_{0,1,\uparrow}> = i\hbar\beta_D L_\omega L_{\omega_2}^{-2}, \tag{32}$$

$$\left|Q_{1,0}\left(\frac{qL_\omega}{\sqrt{2}}\right)Q_{0,0}\left(\frac{qL_\omega}{\sqrt{2}}\right)\right|^2 = \pi^2 e^{-\left(\frac{qL_\omega}{\sqrt{2}}\right)^2}\left(\frac{qL_\omega}{\sqrt{2}}\right)^2, \tag{33}$$

therefore

$$W_R^{\pm}[(0,0,\downarrow)\to(0,0,\uparrow)] = \frac{2\pi^3\hbar\alpha_R^2 L_\omega^2 L_{\omega_1}^{-4}}{(\hbar\omega_1 - g^*\mu_B B)^2}\sum_{\beta,n,\boldsymbol{q}}\left(\frac{qL_\omega}{\sqrt{2}}\right)^2 e^{-\left(\frac{qL_\omega}{\sqrt{2}}\right)^2} \times |\Gamma_\beta^{\pm}(\boldsymbol{q},n)G_\beta(q_{l,n})|^2\delta(g^*\mu_B B \pm \hbar\omega_n^\beta(\boldsymbol{q})), \tag{34}$$

$$W_D^{\pm}[(0,0,\downarrow)\to(0,0,\uparrow)] = \frac{2\pi^3\hbar\beta_D^2 L_\omega^2 L_{\omega_2}^{-4}}{(\hbar\omega_2 - g^*\mu_B B)^2}\sum_{\beta,n,\boldsymbol{q}}\left(\frac{qL_\omega}{\sqrt{2}}\right)^2 e^{-\left(\frac{qL_\omega}{\sqrt{2}}\right)^2} \times |\Gamma_\beta^{\pm}(\boldsymbol{q},n)G_\beta(q_{l,n})|^2\delta(g^*\mu_B B \pm \hbar\omega_n^\beta(\boldsymbol{q})). \tag{35}$$

Taking into account the fact that due to Rashba and Dresselhaus interactions the transition is realized via mediate states $|1,\ 1,\uparrow$ and $|0,2,\uparrow$, respectively, for the transition probability from the state $|0,1,\downarrow$ to the ground state, we get

$$W_R^{\pm}(0,1,\downarrow\to 0,0,\uparrow) = \frac{2^{-1}\pi\hbar\alpha_R^2 L_\omega^2 L_{\omega_1}^{-4}}{(\hbar\omega_1 - g^*\mu_B B)^2}\sum_{\beta,n,\boldsymbol{q}}\left(\frac{qL_\omega}{\sqrt{2}}\right)^4 e^{-\left(\frac{qL_\omega}{\sqrt{2}}\right)^2} \times |\Gamma_\beta^{\pm}(\boldsymbol{q},n)G_\beta(q_{l,n})|^2\delta(\hbar\omega_2 + g^*\mu_B B \pm \hbar\omega_n^\beta(\boldsymbol{q})), \tag{36}$$

$$W_D^{\pm}(0,1,\downarrow\to 0,0,\uparrow) = \frac{4\pi^3\hbar\beta_D^2 L_\omega^2 L_{\omega_2}^{-4}}{(\hbar\omega_2 - g^*\mu_B B)^2}\sum_{\beta,n,\boldsymbol{q}}\left(\frac{qL_\omega}{\sqrt{2}}\right)^4 e^{-\left(\frac{qL_\omega}{\sqrt{2}}\right)^2} \times |\Gamma_\beta^{\pm}(\boldsymbol{q},n)G_\beta(q_{l,n})|^2\delta(\hbar\omega_2 + g^*\mu_B B \pm \hbar\omega_n^\beta(\boldsymbol{q})). \tag{37}$$

Thus, Eq. (34) − (37) give the opportunity to calculate the spin relaxation rate, defined as $T_{21}^{-1} = W^+[(0,0,\downarrow)\to(0,0,\uparrow)] + W^-[(0,0,\downarrow)\to(0,0,\uparrow)]$, and $T_{31}^{-1} = W^+[(0,1,\downarrow)\to(0,0,\uparrow)] + W^-[(0,1,\downarrow)\to(0,0,\uparrow)]$ from the states $(0,\ 0,\downarrow)$ and $(0,\ 1,\downarrow)$ to the ground state, respectively, in 2D QD due to interaction with phonon modes in the phonon cavity for Rashba as well as for Dresselhaus SO interaction.

3. Discussion of results

Calculations are made for a two-dimensional QD created in a GaAs free standing quantum layer using the following values of characteristics of the system: $d = 2\Delta 10^{-7}$ cm, $E_a = 12.42$ eV, $\rho = 5.31$ g/cm^3, $s_l = 5.7\Delta 10^5$ cm/s, $s_t = 3.35\Delta 10^5$ cm/s, $m = 0.067m_0$ [31], $\alpha_R = \beta_D = 2.15\Delta 10^4$ cm/s [22].

1. In Fig. 2 the dependences of spin-flip relaxation rate for transitions from the first excited state to the ground state (T_{21}^{-1}) on magnetic field for Rashba and Dresselhaus SO interactions are presented, when the parabolic confinement energy is $\hbar\omega_0 = 1.1$ meV and T = 3 K. From the obtained results follow that: The magnetic field dependency has allowed and forbidden regions, which is the

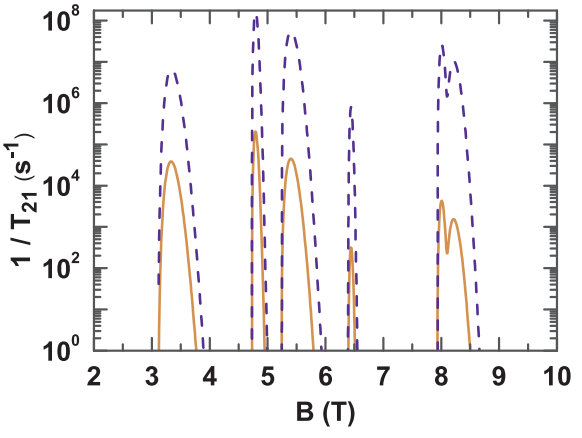

Fig. 2. The dependency of spin relaxation rate T_{21}^{-1} on magnetic field induction for the Rashba coupling (solid lines) and for the Dresselhaus coupling (dashed lines).

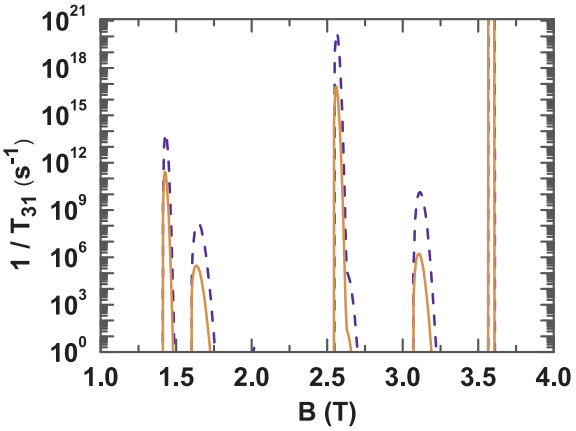

Fig. 3. The dependency of spin relaxation rate T_{31}^{-1} on magnetic field induction for the Rashba coupling (solid lines) and for the Dresselhaus coupling (dashed lines).

consequence of size-quantization of electron as well as phonon states. Indeed, by using Eq. (17), (19), and (21), it is not difficult to verify that $\omega_n \neq 0$ at $q = 0$. Also, numerical calculations show the existence of the gap in the considering range of phonon spectra. Therefore, there are magnetic field values for which don't exist phonon states with energies equal to the energy differences of the Zeeman states. In case of such magnetic fields, the rate of transitions will be zero. As we can see, the spin relaxation rate, depending on magnetic field, can change in a very large region: this fact can be used to have the required rate by means of magnetic field. In allowed regions of transitions for the same values of Rashba and Dresselhaus parameters the relaxation rate caused by H_{so}^{D} substantially exceeds the relaxation rate caused by H_{so}^{R} . Note, however, that these parameters, therefore the relaxation rate, can be governed by the gate-voltages.

In Fig. 3 for the same value of confining energy the magnetic field-dependent curves of relaxation rate T_{31}^{-1} for spin-flip from the state $|0,1,\downarrow\rangle$ to the ground state are presented for the both Rashba and Dresselhaus SO interactions. These results differ from the results in Fig. 2 since the allowed regions dependencies on magnetic induction are distinguished and are relatively narrower. The transition probability in allowed regions has very great values.

The dependency of the spin-flip relaxation rate on parabolic confinement energy for various values of magnetic induction is investigated too. In Fig. 4 the transition rates from the state $|0,0,\downarrow\rangle$ to the ground state for Rashba (line 1) and Dresselhaus (line 2) SO interactions are presented, when $B = 5$T (solid lines) and $B = 10$T (dashed lines), and in Figs. 5 and 6 the transition rates from the state $|0,1,\downarrow\rangle$ to the ground state for Rashba and Dresselhaus SO interaction, respectively, when $B = 0{,}5$T (solid lines) and $B = 2{,}5$T (dashed lines). Note that for Rashba SO interaction, the relaxation rate depending on $\hbar\omega_0$ for transition from first excited state to the ground state has a narrow cusp, which exists on the magnetic dependency curve given in Ref. [22]. For the dependency of relaxation rate from the state $|0,1,\downarrow\rangle$ to the ground state on $\hbar\omega_0$ is typical the same band picture which is shown in magnetic dependency curves for transitions from two excited states to the ground state (Figs. 2 and 3). Such picture is not observed in the $\hbar\omega_0$ -dependency for the relaxation rate when transitions from the first excited state to the ground state occur. As follows from Eq (34)–(37), this behavior is caused by the role of parabolic confinement energy in energy-conversation law: the obtained results show that by means of gate-voltage it is possible to realize the confinement which makes the required transition rate between certain states available.

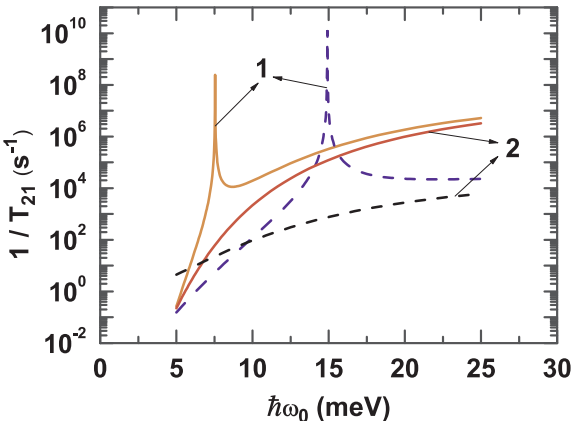

Fig. 4. The dependency of spin relaxation rate T_{21}^{-1} on parabolic confinement energy for the Rashba coupling (lines 1) and for the Dresselhaus coupling (lines 2). $B = 5$T (solid lines), $B = 10$T (dashed lines).

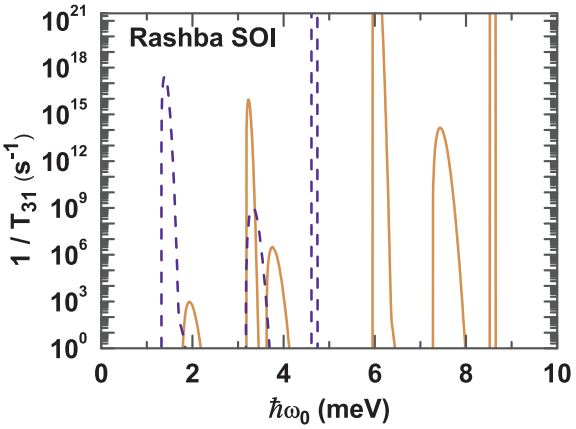

Fig. 5. The dependency of spin relaxation rate T_{31}^{-1} on parabolic confinement energy for the Rashba coupling: $B = 0.5$T (solid lines), $B = 2.5$T (dashed lines).

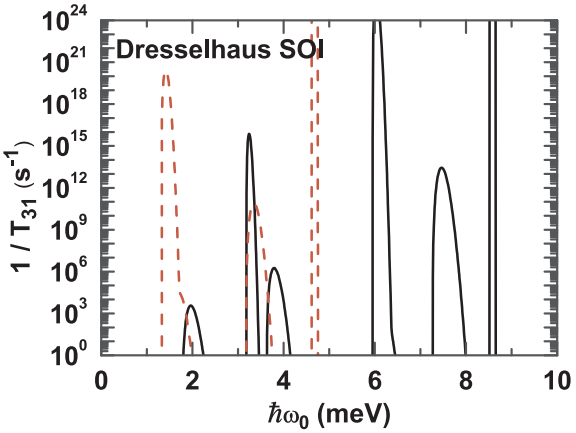

Fig. 6. The dependency of spin relaxation rate T_{31}^{-1} on parabolic confinement energy for the Dresselhaus coupling: $B = 0.5$T (solid lines), $B = 2{,}5$T (dashed lines).

The temperature dependencies of relaxation rates for various values of system parameters and for various SO interactions are studied too (Fig. 7). As we see, in the region of domination of the acoustic phonon modes ($3 - 20$K) the relatively slow rise of the relaxation rate is observed.

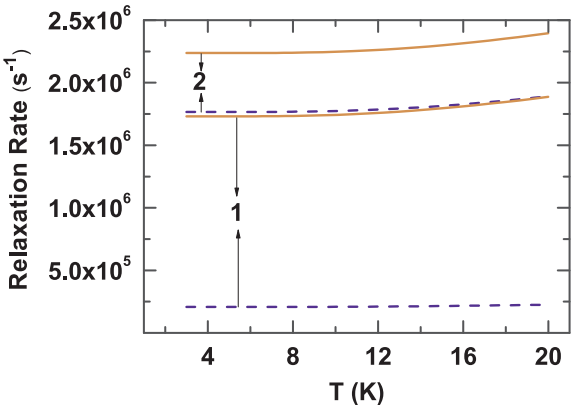

Fig. 7. The dependency of spin relaxation rate from the states $|0,0,\downarrow\rangle$ (lines 1) and $|0,1,\downarrow\rangle$ (lines 2) to the ground state on temperature for the Rashba coupling (solid lines) and for the Dresselhaus coupling (dashed lines) (lines 1: $\hbar\omega_0 = 10$ meV, $B = 5$ T; lines 2: $\hbar\omega_0 = 3.8$ meV, $B = 2.5$ T).

4. Conclusions

In summary, the spin relaxation rate in a two-dimensional quantum dot embedded in a free-standing semiconductor slab in a perpendicular magnetic field has been systematically investigated. Analytical expressions for the relaxation rate caused by the electron scattering on dilatational and flexural acoustical phonon modes have been obtained. The obtained results demonstrate the allowed and forbidden regions of spin relaxation rate as a function of magnetic field. The relaxation rate due to Dresselhaus term substantially exceeds the Rashba term ones. It has been shown that the magnetic field dependent relaxation rate changes in a very large region which can be used to have required rate by means of magnetic field. Also, by means of gate-voltage it is possible to realize the confinement, which makes the required transition rate between certain states available.

Acknowledgements

This work has been supported by State Committee of Science of the Ministry of Education and Science of Armenia (SCS MES RA), within the frame of the research Project No. 15T-1C363.

References

[1] A. Tartakovskii (Ed.), Quantum Dots: Optics, Electron Transport and Future Applications, Cambridge University Press, Cambridge, 2012.
[2] D. Loss, D.P. Divincenzo, Quantum computation with quantum dots, Phys. Rev. 57 (1998) 120–126.
[3] V. Cerletti, W.A. Coish, O. Gywat, D. Loss, Recipes for spin-based quantum computing, Nanotechnology 16 (2005) R27–R49.
[4] S. Datta, B. Das, Electronic analog of the electro-optic modulator, Appl. Phys. Lett. 56 (1990) 665–667.
[5] I. Žutić, J. Fabian, S. Das Sarma, Spin-polarized transport in inhomogeneous magnetic semiconductors: theory of magnetic/nonmagnetic p-n junctions, Phys. Rev. Lett. 88 (2002) 066603.
[6] A. Ebbens, D.N. Krizhanovskii, A.I. Tartakovskii, F. Pulizzi, T. Wright, A.V. Savelyev, M.S. Skolnick, M. Hopkinson, Optical orientation and control of spin memory in individual InGaAs quantum dots, Phys. Rev. B 72 (2005) 073307.
[7] E. Poem, O. Kenneth, Y. Kodriano, Y. Benny, S. Khatsevich, J.E. Avron, D. Gershoni, Optically induced rotation of an exciton spin in a semiconductor quantum dot, Phys. Rev. Lett. 107 (2011) 087401.
[8] R. Hanson, L.P. Kouwenhoven, J.R. Petta, S. Tarucha, L.M.K. Vandersypen, Spins in few-electron quantum dots, Rev. Mod. Phys. 79 (2007) 1217–1265.
[9] D. Rugar, R. Budakian, H.J. Mamin, B.W. Chui, Single spin detection by magnetic resonance force microscopy, Nature (London) 430 (2004) 329–332.
[10] J.M. Elzerman, R. Hanson, L.H. Willems van Beveren, B. Witkamp, L.M.K. Vandersypen, L.P. Kouwenhoven, Single-shot read-out of an individual electron spin in a quantum dot, Nature (London) 430 (2004) 431–435.
[11] M. Kroutvar, Y. Ducommun, D. Heiss, M. Bichler, D. Schuh, G. Abstreiter, J.J. Finley, Optically programmable electron spin memory using semiconductor quantum dots, Nature (London) 432 (2004) 81–84.
[12] K.C. Nowack, F.H.L. Koppens, YuV. Nazarov, L.M.K. Vandersypen, Coherent control of a single electron spin with electric fields, Science 318 (2007) 1430–1433.
[13] A.V. Khaetskii, Y.V. Nazarov, Spin relaxation in semiconductor quantum dots, Phys. Rev. B 61 (2000) 12639.
[14] A.V. Khaetskii, Y.V. Nazarov, Spin-flip transitions between Zeeman sublevels in semiconductor quantum dots, Phys. Rev. B 64 (2001) 125316.
[15] V.N. Golovach, A. Khaetskii, D. Loss, Phonon-induced decay of the electron spin in quantum dots, Phys. Rev. Lett. 93 (2004) 016601.
[16] S. Amasha, K. MacLean, Iu Radu, D.M. Zumbuhl, M.A. Kastner, M.P. Hanson, A.C. Gossard, Electrical control of spin relaxation in a quantum dot, Phys. Rev. Lett. 100 (2008) 046803.
[17] T. Meunier, I.T. Vink, L.H. Willems van Beveren, K.-J. Tielrooij, R. Hanson, F.H.L. Koppens, H.P. Tranitz, W. Wegscheider, L.P. Kouwenhoven, L.M.K. Vandersypen, Experimental signature of phonon-mediated spin relaxation in a two-electron quantum dot, Phys. Rev. Lett. 98 (2007) 126601.
[18] D.M. Frenkel, Spin relaxation in GaAs-$Al_xGa_{1-x}As$ heterostructures in high magnetic fields, Phys. Rev. B 43 (1991) 14228–14231.
[19] A.J. Pearce, G. Burkard, Electron spin relaxation in a transition-metal dichalcogenide quantum dot, 2D Mater. 4 (2017) 025114.
[20] D. Heiss, S. Schaeck, H. Huebl, M. Bichler, G. Abstreiter, J.J. Finley, D.V. Bulaev, D. Loss, Observation of extremely slow hole spin relaxation in self-assembled quantum dots, Phys. Rev. B 76 (2007) 241306 (R).
[21] M. Trif, P. Simon, D. Loss, Relaxation of hole spins in quantum dots via two-phonon processes, Phys. Rev. Lett. 103 (2009) 106601.
[22] D.V. Bulaev, D. Loss, Spin relaxation and anticrossing in quantum dots: Rashba versus Dresselhaus spin-orbit coupling, Phys. Rev. B 73 (2005) 205324.
[23] Y.Y. Liao, Y.N. Chen, D.S. Chuu, T. Brandes, Spin relaxation in a GaAs quantum dot embedded inside a suspended phonon cavity, Phys. Rev. B 71 (2005) 205324.
[24] M. Grimsditch, R. Bhadra, I.K. Schuller, Lamb waves in unsupported thin films: a brillouin-scattering study, Phys. Rev. Lett. 58 (1987) 1216–1219.
[25] R. Bhadra, M. Grimsditch, I.K. Schuller, F. Nizzoli, Brillouin scattering from unsupported Al films, Phys. Rev. B 39 (1989) 12456–12459.
[26] M.D. Williams, S.C. Shunk, M.G. Young, D.P. Docter, D.M. Tennant, B.I. Miller, Fabrication of free-standing quantum wells, Appl. Phys. Lett. 61 (1992) 1353–1354.
[27] D.M. Zumbühl, J.B. Miller, C.M. Marcus, K. Campman, A.C. Gossard, Spin-orbit coupling, antilocalization, and parallel magnetic fields in quantum dots, Phys. Rev. Lett. 89 (2002) 276803.
[28] R.S. Deacon, Y. Kanai, S. Takahashi, A. Oiwa, K. Yoshida, K. Shibata, K. Hirakawa, Y. Tokura, S. Tarucha, Electrically tuned g tensor in an InAs self-assembled quantum dot, Phys. Rev. B 84 (2011) 041302 (R).
[29] N. Bannov, V. Mitin, M. Stroscio, Confined acoustic phonons in a free-standing quantum well and their interaction with electrons, Phys. Status Solidi B 183 (1994) 131–142.
[30] F.F. Fang, W.E. Howard, Negative field-effect mobility on (100) Si surfaces, Phys. Rev. Lett. 16 (1966) 797–799.
[31] S. Adachi, GaAs, AlAs, and $Al_xGa_{1-x}As$: material parameters for use in research and device applications, J. Appl. Phys. 58 (1985) R1–R29.